Rocket Vehicule for a 4Kg Payload

Team 49 Project Technical Report for the 2021 Latin American Space Challenge

David E. Becerra-Sierra[1], Joan S. Villalba[2], Oscar I. Ayala[3] ,Santiago H. Rincon[4], Juan M. Vivas[5] and Julián Rodríguez-Ferreira[6]
Universidad Industrial de Santander, Bucaramanga, Colombia, 680002

This document is the summary of the Orion Rocket design Process, Orion rocket will reach an altitude of 3 kilometers and will carry a payload of 4 Kilograms, It will also carry an unmanned aerial vehicle that will be ejected at 500 m altitude. the rocket propulsion is a 3 grain Solid rocket propellant motor L1915, KNSB is used as the propellant. a 3ft area drogue parachute will be deployed at apogee and the main 8ft area parachute will be deployed at 500 m height, providing a descent velocity of around 6 m/s. The rocket counts with robust avionics and redundant electronics to control the different events that occur during the mission, in addition to the visualization through a graphic interface developed by the team members.

Nomenclature

$LASC$	=	Latin American Space Challenge
$KNSB$	=	potassium nitrate and sorbitol mix
$KNO3$	=	potassium nitrate
$SCUA$	=	Semillero de Coheteria UIS Aeroespacial
CO_2	=	Carbon Dioxide
GPS	=	Global Positioning System
$I2C$	=	Communication protocol
MCC	=	Mission Control Center
SPI	=	Communication Protocol
$UART$	=	Communication Protocol
$GPIO$	=	General Purpose Input/Output
$APOGEE$	=	the high point of a flight

I. Introduction

Since 2017 SCUA, Semillero de Coheteria UIS Aeroespacial, have been one of the most active seedbeds in Colombia, working with a lot of economic and social constraints SCUA students have reached a lot of important goals, individual and collective talking, LASC 2022 in one of these important goals that students are trying hard to achieve, Orion Rocket will reach an altitude of 3 kilometers and will carry a payload of 4 Kilograms, It will also carry an unmanned aerial vehicle that will be ejected at 500 m altitude.

[1]Mechanical Engineering , Escuela de Ingeniería Mecánica, david.becerra2@correo.uis.edu.co.
[2]Undergraduate, Escuela de Ingeniería Mecánica, JOAN.VILLALBA@correo.uis.edu.co
[3]Undergraduate, Escuela de Ingeniería Mecánica, oscar2172249@correo.uis.edu.co
[4]Undergraduated, Escuela Ingeniería Elétrica, Electrónica y de Telecomunicaciones, santiago981024@gmail.com
[5]Graduate Student, Escuela de Ingeniería Eléctrica, Electrónica y de Telecomunicaciones, juan21624860@correo.uis.edu.co.
[6]Professor, Escuela de Ingeniería Eléctrica, Electrónica y de Telecomunicaciones, jgrodrif@uis.edu.co.

II. System Architecture Overview

A. Propulsion System

Propulsion system is the most critic inside a rocket mission, unless it properly works, none of the other systems will perform, the motor for LASC 2022 is a solid propellant motor, the grain is made of KNO3 and sorbitol, 65-35 respectively.

1. Methodology

after a state of the art review, taking pieces of different works, a base code was created with the purpose of designing from scratch a solid rocket motor, the flow diagram is shown in figure 1, the first step in order to design a rocket motor is the capability of selecting and determine the independent variables, this variables are the base of the design, with these input it is possible to work with the propulsion equations to get the dependent variables, then get a solid design and come back to the independent variables if adjustments are needed.

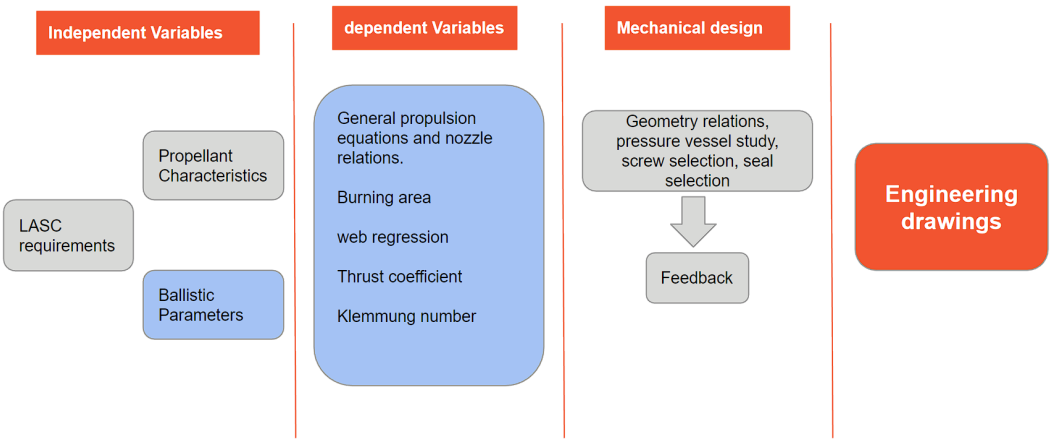

Fig. 1 Methodology

2. Independent variables

there are 2 independent variable fields, the first one taking into account is the propellant chemistry and performance characteristics, an early selection of the propellant that is going to be used for the grain can be made, this selection depends on the availability of the components on your local market, on the expertise you have handling an specific mix, handling safety, among others. The principal characteristics of the propellant are: burn rate, density, ratio of specific heats and specific impulse. These are the independent variables to consider.

The second one is an integration between the mission requirements and a ballistic study, the first step is to determine the apogee goal, the average rocket total weight, the rocket desire envelope and the environmental conditions, these data is used to fill a dynamic flight calculation, not so robust, and with the help of propulsion equations and the selection of a burn time, the average thrust and total impulse are obtained.

3. Design process

The first step is to get the burning area,the value through the time of the burning area depends on the web regression, and the web regression depends on the burning time, burning area can be expressed as a time variable doing some arranges.

with the burning area, the propellant density and the propellant burning rate, the mass flow can be calculated, it is integrated and dived by the burning time, then we can get an average mass flow value.

Another dependent value that is calculated is the thrust coefficient, with this, the characteristic propellant velocity, he gravity and an efficiency coefficient the specific impulse is obtained. With the specific impulse and the mass flow, we can get the thrust, and this is the input variable.

Thus the grain length is calculated having already the outside diameter and the core diameter. An important variable is the nozzle throat, and we get this with the help of richar nakka experimental klemung charts, klemung number is the ratio between the max burning area and the throat area, using 1000 PSI as the design pressure, a KN of 420 is given, and we can get the throat diameter with this process.

Next step is to select the case material and the wall thickness, the selected material was 304 stainless steel and the wall thickness was calculated using pressure vessel equations.

the final step is to assure the system sealing, seals were selected using the Parker o-ring manual.

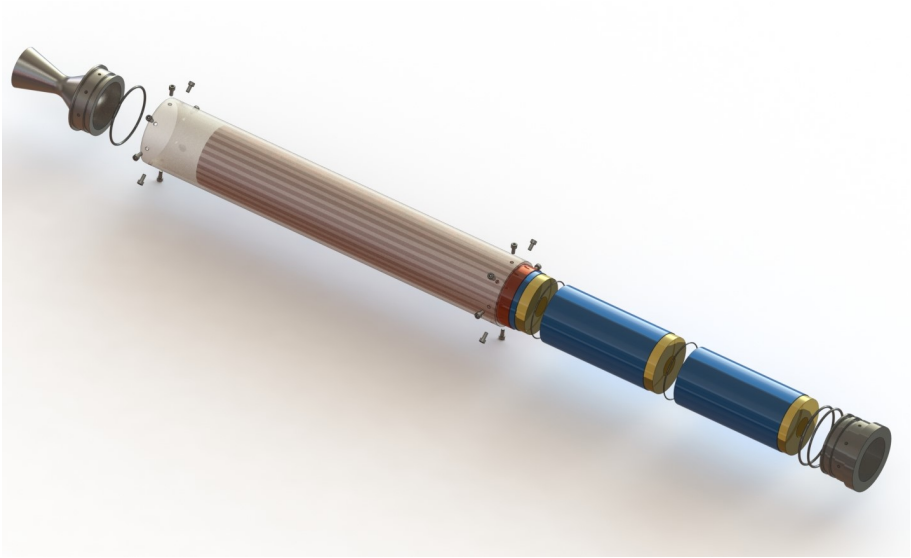

Fig. 2 Motor distribution

4. Motor distribution

The rocket motor consist of 3 propellant grains separates with o-rings to prevent grain failures, those grains are melted inside a 3d printed cast designed by SCUA, the grains are covered with cardboard and all three grains are aligned inside a linear, that linear fits inside the steel case and with the help of a bolted joint and seal, the system is closed and safe.

.

B. Structural System

The structural design was based in the *Design for Manufacturing and Assembly (DMA)* methodology, this means that the manufacturing and assembly process was a critical point decision though all the aerodynamics and mechanical design.

The structural subsystem of the *Orion Rocket* was thinking for additive manufacturing and easy assembly, the final result is ilustrated in the figure 3

Fig. 3 Orion Rocket Render

The section II.E will discuss further the mechanical issues and how was solved it, it is not shown but, the external surface of the rocket has a resin protection for the high temperatures that it could reach,

The rocket structure is divided into four parts as the table 1 shows:

Table 1 Structural Components

Part	Description
Ogive	Roundly tapered end of the rocket
Body Frame	Shell when the Avionics, CANSAT, and recuperation System are.
Principal Coupling Ring (PCR)	The body Frame, Motor Frame, and motor are attached to it
Motor Frame	Shell when the motor and fins are placed
Rack	Cilindrical structure used for the assembly of the body Frame and Rocket components

C. Aerodynamics

The aerodynamic design was made using *OpenRocket Software* which use the Barrowman Method for the Normal Force Coefficient and center pressure distance calculations.
The design was iterative and was based in the following performance parameters

- $Apogee >= 3000m$
- $Stability \in [1-3]$
- $mass < 15Kg$

Dynamically stability was not analyzed, nevertheless the variations due to the burn of the propellant and angle of attack was count in the design, figures 4 and the table **??** resumes the design.

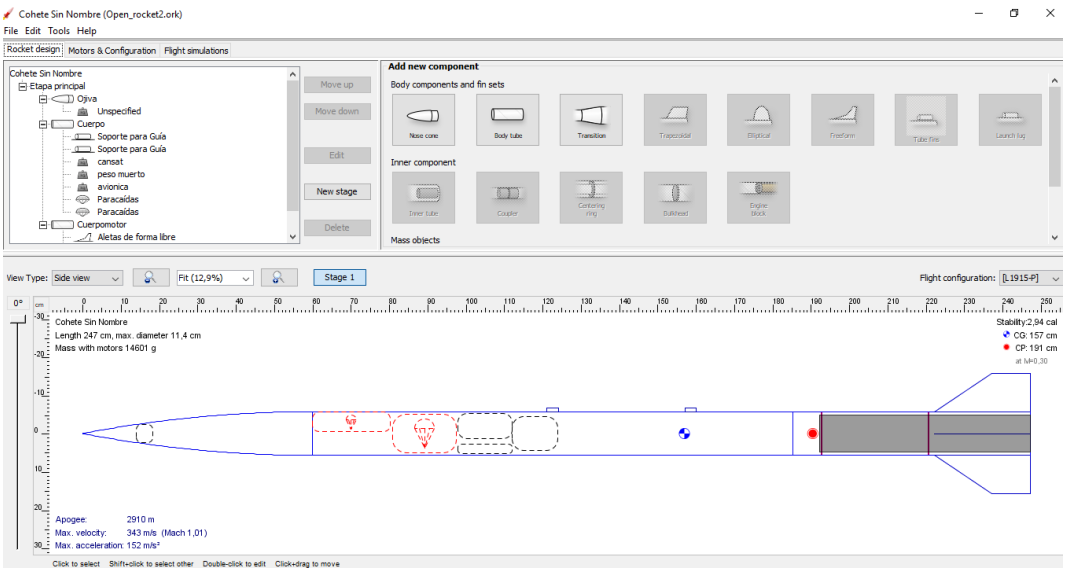

Fig. 4 OpenRocket Software Design

The rocket has an external diameter of 11.4 cm and a total longitude of 247 cm with the ogive included.

Table 2 Aerodynamic Coefficients with Angle of Attack of 10°

Structural Aerodynamics			
Component	C_{NO}	C_D	X_{PC} **[cm]**
Ogive	2,84	0,05	27,90
Body Frame	2,66	0,17	123,00
Motor Frame	1,32	0,12	216,00
Fins	-	0,10	233,00

The calcultaions was performed for 10° of Angle of Attack, this was an input for the structural design of the rocket, beaing at this point the maximum loads on the surface of the rocket.

In order to made the rocket stable was necessary to put a ballast mass at the tip of the rocket,inside the ogive, this is what in the figured 4 is named as Unspecified.

D. Internal Configuration

In order to maintain an easy assembly and additive manufacturing was obligatory to split the body frame into three parts as continues:

- Expulsion frame
- CANSAT frame
- Avionics Frame

In next sections the mechanical design will be discussed, but what here concerns the coupling methods and divisions systems will be presented. A general overview is ilustrated in the figure 5

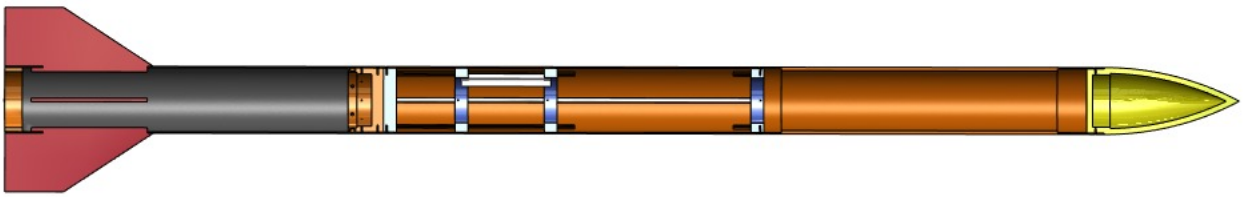

Fig. 5 Internal Configuration Overview

Here the ogive was just ilustrative, the real dimensions are shown in 3 and has a real longitud of 60 cm. The figure 5 shows what is the role of the rack, and the double mean of the rings rack, as is shown in the figure, the rings are structural supports for the frame, but also, are points of assembly through 3mm bolts, for every body frame part, there is a ring which it is supported. in the figure 6b and 6a the coupling between the fins, ogive and airframe is shown.

(a) Fin coupling to the Motor Frame **(b)** $y = 5/x$

Fig. 6 Ogive Coupling to the Body Frame

E. Structural Design

The structural design of the rocket was made thinking in the low strength of the PLA material (used in Additive Manufacturing) Therefore, The rigidity and structural stability were improved through thickness and geometry enhacement. The principal enhacements was the modification of the cross area of the body as the figure 7 shows.

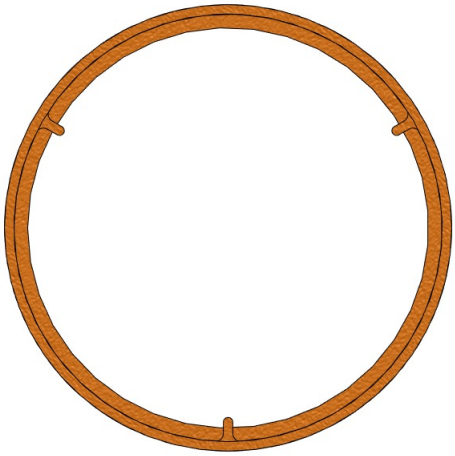

Fig. 7 Body and Motor Frames cross sections

The bodyFrame is also supported by the supported rings of the rack, to made the rack the masterpiece for the assembly the rings was modified as the figure 8 shows.

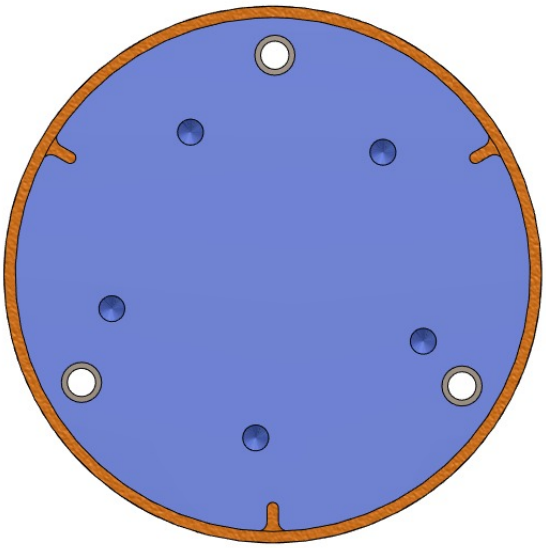

Fig. 8 Caption

The final cricital point in the design was the motorFrame and bodyFrame attachments, this is the part which tasmit the power of the combustion to the structural rocket, therefore is a critical point in the design and assembly, this part is known in the Orion rocket as *Coupling principal ring*, and is shown in the figure **??**

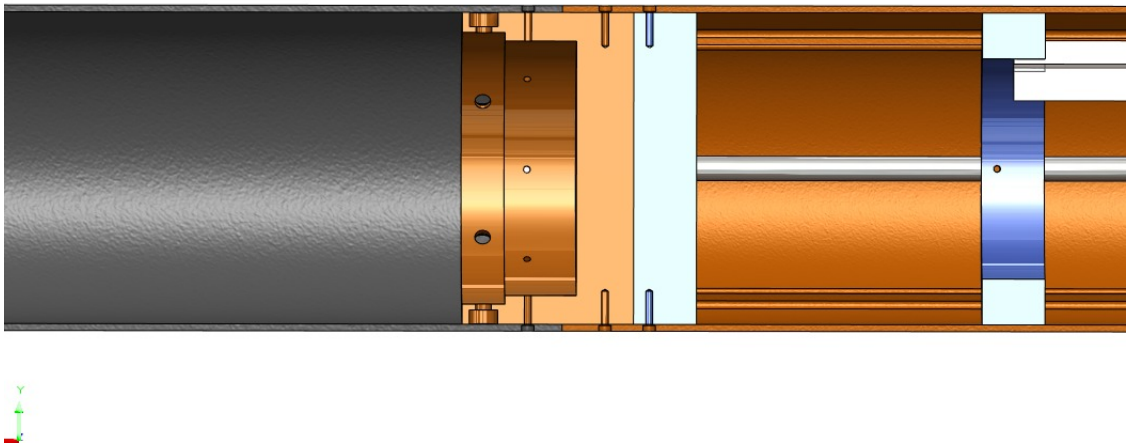

Fig. 9 Principal ring attachment

Here, is shown how the body frame, the motor, and the motor frame are coupling together, this piece was made of composite material known as Onix which it has carbon fiber reforcement.

F. Subsystems coupling

The subsystems coupling was the final design point in the structural design, here is shown the principal coupling which is the CANSAT expulsion system, this represent a challenge due to the cinematics of the expulsion, which will be laterally.

Expulsion system assembly:

The cansat ejection mechanism is composed of a tension subsystem, which consists of two elastic bands attached to two rods of the rocket rack, and the release subsystem, which consists of two rods attached to the cam of an SG90 microservo, which in turn and initially block the opening of the windows by means of a clamping piece which is screwed to the opening surface that pivots at the end of the square perforation that will carry the rocket body.

Fig. 10 Expulsion system assembly.

1. Tension subsystem

The cansat cylinder is tensioned by means of an elastic band attached to two of the bars of the rocket rack. In its initial position it will keep accumulated a potential energy that will be used after the release of the pins provided by the upper and lower hooks of the release mechanism.

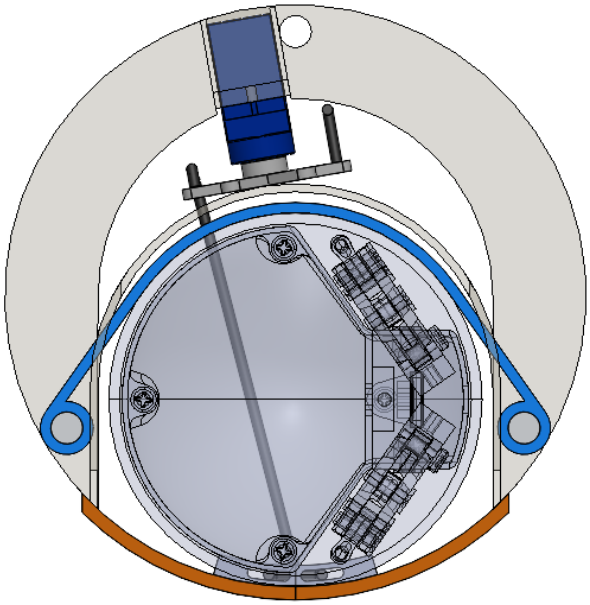

Fig. 11 Tensioned rubber band configuration.

2. Release subsystem

The SG90 microservo is in charge of transmitting the rotation of the motor to the bar, making it move horizontally and vertically. For practical purposes these bars will be called upper hook and lower hook as illustrated in the figure.

As a result, when actuating the servo rotation counterclockwise, as illustrated in the image, the clamping parts will be free of pins and the potential energy accumulated by the voltage subsystem will be the one that will allow the output of the cansat.

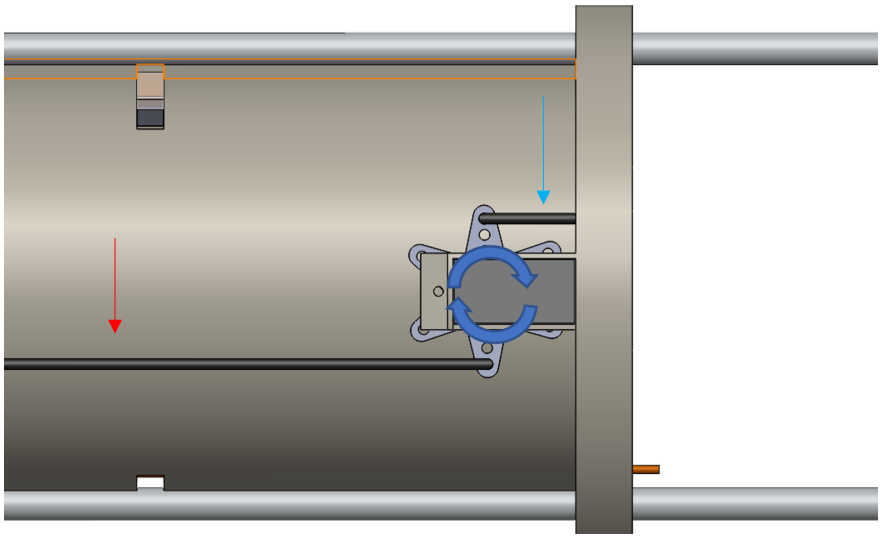

Fig. 12 Servomotor drive.

The blue and red arrows indicate the upper and lower hook, respectively.

G.

H. Recovery System

System overview:

The recovery system was designed using CO2 pipes, a CO2 ejection case was designed by the SCUA students, the gas will pressurize the space between the nozzle and the recovery system plate, the PLA bolts will break and the nozzle will be ejected from the body, the green plate will also be ejected thanks to the cord union, then it will be attached to the 3 ft area drogue parachute that will be deploy at apogee.

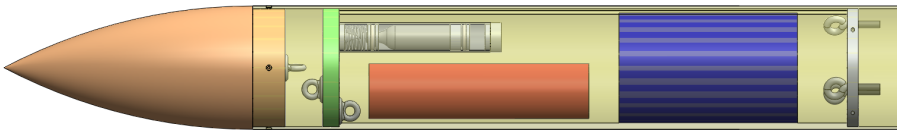

Fig. 13 Main recovery system

Later at 500 m height, the main parachute, a standard 8ft area parachute will be deployed, using a servomotor unlock device as the one used before.

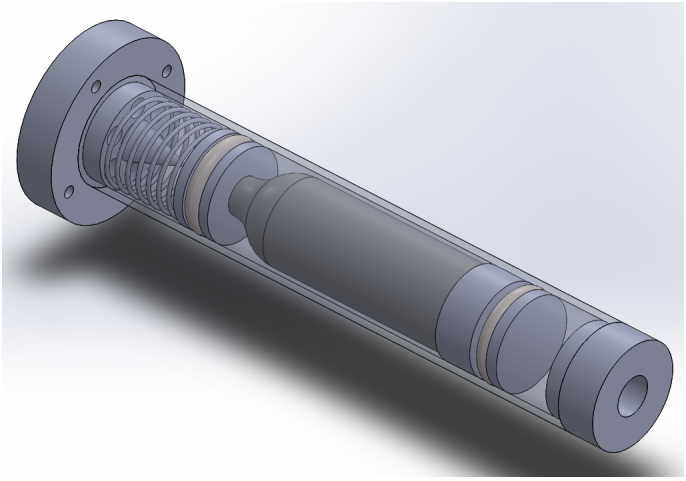

Fig. 14 CO2 ejection device.

Figure shows the designed system, the CO2 pipe will be attached to 2 racetracks, the first impulse will be given with a signal that is going to fire a powder cord that is going to move the system, then a tip is going to rip the pipe membrane, the spring is going to move the pipe back and the gas will flow through the holes.

I. Avionics

The mission of the ORION-UIS rocket developed by the SCUA team will be controlled through the avionics developed by the team members. This avionics is composed of 6 different stages: main flight electronics (flight computer), power stage, redundant electronics, telemetry and transmission, control stage and ground station. The general block diagram can be seen in Figure 15

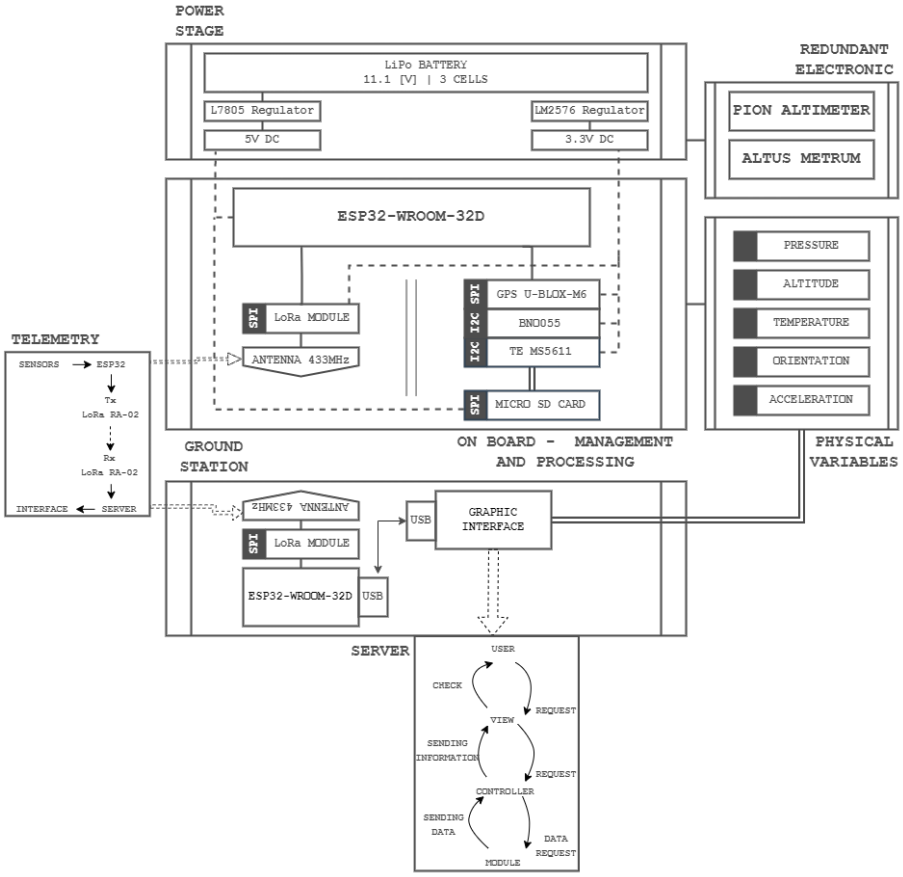

Fig. 15 General block diagram.

Based on the objectives of the mission and especially the objectives of the Avionics subsystem, it will be necessary to obtain measurements through different sensors of variables such as: atmospheric pressure, temperature, orientation, acceleration, geographic position and finally altitude. The latter will be essential for the control stage.

*1. **Physical variables***

To define the physical variables that will be sensed during the mission, the measurements that are necessary and serve as actuators for the correct operation of the avionics subsystem and other subsystems that depend on a specific physical variable for its activation. were taken into account. Taking into account the above, the physical variables that will be measured and stored are:

- **Temperature:** With the measurement of this variable, the aim is to characterize the temperatures recorded during the flight and additionally to make a later comparison with the ambient temperatures taken at the site. Additionally, the temperature variable is used to add precision to the altitude calculation through the selected sensor. The respective units for this variable will be degrees Celsius [°C].

- **Atmospheric pressure:** This variable is one of the most relevant and important variables of the mission. Initially, the aim is to have a comparison of the pressures recorded during the mission and on the other hand the calculation of the height reached by the vehicle will be estimated by the atmospheric pressure: Since as the height increases the pressure decreases it is possible to perform this calculation. The respective unit of this variable will be the bar [B].

- **Altitude:**In terms of the mission, altitude is the most important physical variable because different mechanical actions and vehicle characterization depend on it. The altitude is the result of operating the physical variables of pressure and temperature. With this result it is sought to know the altitude of the rocket in real time throughout

the mission, also, as mentioned previously, will be crucial for the activation of the recovery system because it will be one of the alternatives used for the apogee detection of the rocket. The respective units of altitude will be in meters [m].

- **Acceleration:** The nature of the vehicle determines that the accelerations in the 3 different degrees of freedom will be of great importance in the ORION-UIS mission. By measuring this variable the control of decisive tasks during the mission is performed, among the most important tasks are: to know the direction of flight of the rocket, it will help to differentiate the different flight stages during the mission and finally the apogee detection. The units of this variable are: [m/S2].

- **Orientation**: With the measurement of this variable it is sought to have knowledge of the rocket orientation during each of the flight stages, this knowledge will allow to take actions of flight correction in case they are necessary. Additionally, it will be useful in the characterization and post-processing of data taken during the mission. The units of measurement will be degrees [°].

- **Geographical Position:**In terms of the mission, the geographical position of the vehicle is indispensable since in this way it is possible to recover the vehicle once the mission is over, likewise, it is possible through the processing of the data obtained to make a two-dimensional estimation of the rocket's behavior. This variable will be measured in geographic coordinates.

*2. **Main flight electronics***

The main avionics will consist of a flight computer designed by the team members. This flight computer bases its processing on an ESP32 microcontroller, which, through peripherals and serial communication protocols such as I2C, UART and SPI is able to control actuation signals through its GPIO ports. The main objective of the flight computer is to control, characterize and report the status of the mission, for this purpose it performs the sensing of the variables mentioned in the previous section, this is achieved through the barometric pressure sensor, IMU inertial measurement unit and GPS satellite locator. On the other hand, it is in charge of storing in SD memory and transmitting to the ground station the data obtained from the sensors through the LoRa communication protocol using the 433 MHz frequency band legally usable for amateur purposes. Finally, a processing of the received data will be implemented at the ground station and displayed at the mission control center (MCC). The technical specifications of each device used can be visualized in Table 3 and Table 4, as well as its energy consumption characteristics can be visualized in Table 5.

Device reference	Protocol	Range	Sensitivity tolerance	
			Typical	Maximum
BNO055 - Accelerometer	I2C	±2g | ±4g | ±8g | ±16g	±1 %	±4 %
BNO055 - Gyroscope	I2C	125°/S | 250°/s | 500°/s | 1000°/s | 2000°/s	±1 %	±3 %
BNO055 - Magnetometer	I2C	Brg,xy: ±1300 µT | Brg,z: ±2500 µT	±5 %	±8 %
MS5611 - Pressure	I2C	10 - 1200 [mbar]	-	±1.5 [mbar]
MS5611 - Temperature	I2C	-40 to +85 [°C]	-	±0.8 [°C]

Table 3 Sensors features

Device reference	Protocol	Horizontal position accuracy	Maximum update rate
U-blox NEO-6M	UART	2.5m	5Hz

Table 4 Technical features of the GPS module.

3. ***Power supply stage***

A power consumption study was performed for each device used in the avionics, which can be seen in Table 5. It was estimated that a 3-cell battery at 11.1V of 1000mAh is sufficient to power all the devices to be used in the subsystem. In conjunction. Once the sufficient power supply for the subsystem has been ensured. As can be seen in Figure 15 of the general diagram, it will be essential to have 2 stable voltage levels, 3.3V and 5V, this will be achieved through the voltage regulator MP2307.

Device reference	O. Voltage [V]	O. Current [mA]	Quantity	Current Consumption [mA]
ESP32-WROOM-32D	3,3	150	1	150
BNO055	3,3	12,3	1	12,3
TE-MS5611	3,3	0,0125	1	0,0125
U-blox NEO-6M	3,3	45	1	45
Transceiver LoRa Ra-02	3,3	120	1	120
Pyro (Stand-by)	3,3	1	2	2
SD Card socket	5	40	1	40
ESPCAM - module	5	180	1	180
Approximate total current consumption				549,3125

Table 5 Electrical features of the devices.

4. ***Telemetry stage***

As previously mentioned, the data acquired by the sensors and the mission status can be visualized on the ground and stored locally in a SD memory. For data transmission, LoRa Ra - 02 modules will be used, which are based on SX1278 transceiver modules. These modules were chosen due to the practicality, robustness and functionality they offer, because in a simple way it is possible to establish a point to point radio link of up to 10Km, which is more than enough within the characteristics of the mission (3Km). The operation of these modules has been previously validated through a distance validation test carried out in the city of Bucaramanga, Colombia where it was possible to establish a point-to-point radio link of approximately 6.62Km (Figure 16) by sending data packets large enough to simulate the data coming from the sensors. The test was carried out using 433MHz frequency and 3dBi gain omnidirectional antennas.

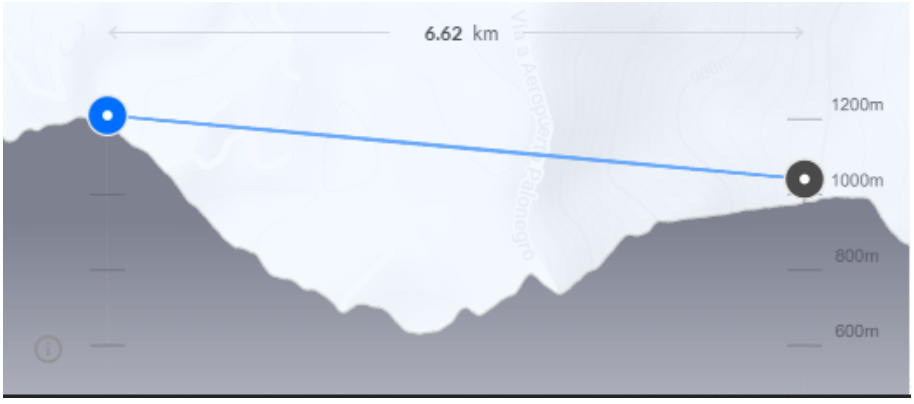

Fig. 16 Radio link distance ensured with LoRa modules.

Device reference	Protocol	Range	Specifications	
			frequency band	transmition power
LoRa Ra-02(SX1278) - Radio	Half-duplex SPI	±10km	433MHz	20dBm
Antenna Lora SMA - Antenna	SPI	-	433MHz	3dBi

Table 6 LoRa module features.

5. ***Ground station***

The block diagram of the ground station can be visualized in Figure 15 in the ground station section, which will base its operation on an ESP32 microcontroller, will establish communication through the radio link with the LoRa Ra - 02 module and will provide the received data to the local server through the serial port. Finally the data will be displayed in real time on the local server which will be built based on frameworks with the Python programming language. The electrical characteristics of the devices can be visualized in Table 5 and Table 6.

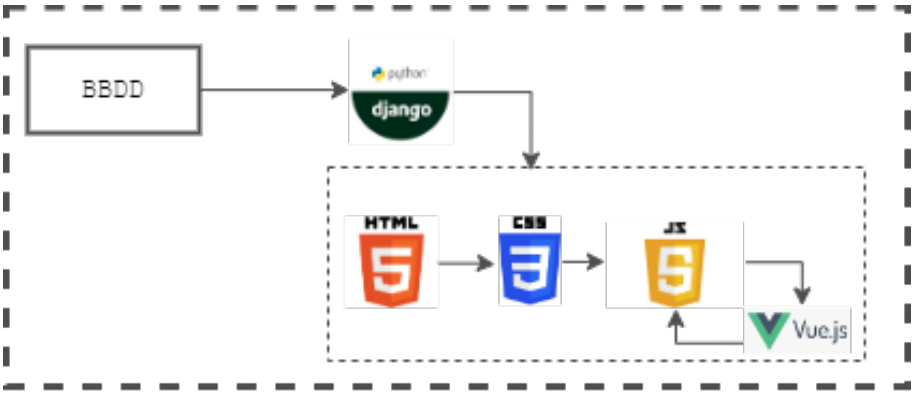

Fig. 17 Techonologies used for Graphic Interface.

6. ***Redundant Electronics***

The redundant electronics will be supported by a COTS altimeter device validated by the event sponsors. Additionally, in parallel to the main flight computer, there will be an electronic system sufficiently accurate to determine the critical moments of the mission, especially the apogee, so that in case of any failure in the main system, the redundant electronics will have the power to perform the immediate activation of the system. The above described is valid for the 2 activation events of the recovery system. The basic block diagram can be seen in Figure 18. Additionally, the electrical characteristics of these devices can be found in Table 3 and Table 5.

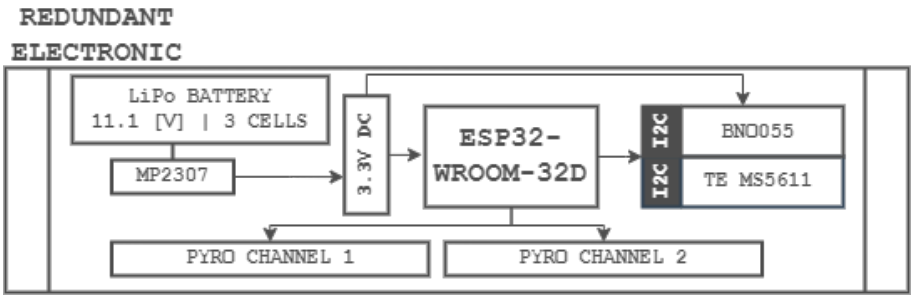

Fig. 18 Redundant electronics designed.

III. Mission Concept of Operation Overview

IV. Conclusions and Lessons Learned

- most important lesson is that the communication of the design process between the subsystems is the key, working as a co-working company, having good communication channels and everything organized are some of the most important practice to achieve a goal.
- To get help from governmental and public institutions is a most when a project of this caliber is planned in a developing country, a lot of obstacles are always on the way to success.
- It was determined that the frequency of operation of the microcontroller is fundamental in the design of the avionics since being a short duration event and with several eventors within itself the best option is a fast processing. In the case of the ORION-UIS equipment, the ESP32 microcontroller was chosen, which is more than enough.
- For the choice of the communication system it is necessary to validate the range, the different operating modes of the radio and the different types of antennas under real conditions to ensure the least possible loss of information and the correct transmission of data.

References

[1] Soyer, S., "Small space can: CanSat," *Proceedings of 5th International Conference on Recent Advances in Space Technologies - RAST2011*, 2011, pp. 789–793. https://doi.org/10.1109/RAST.2011.5966950.

[2] Kizilkaya, M. Ö., Oğuz, A. E., and Soyer, S., "CanSat descent control system design and implementation," *2017 8th International Conference on Recent Advances in Space Technologies (RAST)*, 2017, pp. 241–245. https://doi.org/10.1109/RAST.2017.8002947.

[3] Tanaka, M., Tanaka, K., and Wang, H. O., "Practical Model Construction and Stable Control of an Unmanned Aerial Vehicle With a Parafoil-Type Wing," *IEEE Transactions on Systems, Man, and Cybernetics: Systems*, Vol. 49, No. 6, 2019, pp. 1291–1297. https://doi.org/10.1109/TSMC.2017.2707393.

[4] Celebi, M., Ay, S., Ibrahim, M. K., Aydemır, M. E., Bensaada, M., Fernando, L. H. J. D. K., Akiyama, H., and Yamaura, S., "Design and navigation control of an advanced level CANSAT," *Proceedings of 5th International Conference on Recent Advances in Space Technologies - RAST2011*, 2011, pp. 752–757. https://doi.org/10.1109/RAST.2011.5966942.

[5] Meiga, A., "Eagle bird logo," , 2022. URL https://www.vecteezy.com/vector-art/3456052-eagle-bird-logo, vecteezy.

[6] Jimenez, A., and Icaza, D., "Thrust Vectoring System Control Concept," *IFAC Proceedings Volumes*, Vol. 33, 2000, pp. 235–244. https://doi.org/10.1016/S1474-6670(17)35476-9.

[7] Ramadhan, R. P., Ramadhan, A. R., Putri, S. A., Latukolan, M. I. C., Edwar, and Kusmadi, "Prototype of CanSat with Auto-gyro Payload for Small Satellite Education," *2019 IEEE 13th International Conference on Telecommunication Systems, Services, and Applications (TSSA)*, 2019, pp. 243–248. https://doi.org/10.1109/TSSA48701.2019.8985514.

[8] Kwak, J., and Sung, Y., "Autonomous UAV Flight Control for GPS-Based Navigation," *IEEE Access*, Vol. 6, 2018, pp. 37947–37955. https://doi.org/10.1109/ACCESS.2018.2854712.

[9] Ajanic, E., Feroskhan, M., Mintchev, S., Noca, F., and Floreano, D., "Bioinspired wing and tail morphing extends drone flight capabilities," *Science Robotics*, Vol. 5, No. 47, 2020, p. eabc2897. https://doi.org/10.1126/scirobotics.abc2897.

[10] Di Luca, M., Mintchev, S., Heitz, G., Noca, F., and Floreano, D., "Bioinspired morphing wings for extended flight envelope and roll control of small drones," *Interface Focus*, Vol. 7, 2017. https://doi.org/10.1098/rsfs.2016.0092.

[11] Burgess, S., "A review of linkage mechanisms in animal joints and related bioinspired designs," *Bioinspiration &amp Biomimetics*, Vol. 16, No. 4, 2021, p. 041001. https://doi.org/10.1088/1748-3190/abf744.

[12] Meyers, R. A., "Comparative anatomy of the postural mechanisms of the forelimbs of birds and mammals," *Journal of Ornithology*, Vol. 160, No. 3, 2019, pp. 869–882. https://doi.org/10.1007/s10336-019-01678-3, URL https://doi.org/10.1007/s10336-019-01678-3.

[13] Jitsukawa, T., Adachi, H., Abe, T., Yamakawa, H., and Umezu, S., "Bio-inspired wing-folding mechanism of micro air vehicle (MAV)," *Artificial Life and Robotics*, Vol. 22, No. 2, 2017, pp. 203–208. https://doi.org/10.1007/s10015-016-0339-9, URL https://doi.org/10.1007/s10015-016-0339-9.

[14] Stowers, A. K., Matloff, L. Y., and Lentink, D., "How pigeons couple three-dimensional elbow and wrist motion to morph their wings," *Journal of The Royal Society Interface*, Vol. 14, No. 133, 2017, p. 20170224. https://doi.org/10.1098/rsif.2017.0224, URL https://doi.org/10.1098/rsif.2017.0224.

[15] Burgess, S., Lock, R., Wang, J., Sattler, G., and Oliver, J., "The Energy Benefits of the Pantograph Wing Mechanism in Flapping Flight: Case Study of a Gull," *International Journal of Micro Air Vehicles*, Vol. 7, No. 3, 2015, pp. 275–283. https://doi.org/10.1260/1756-8293.7.3.275.

[16] Pennycuick, C., *Modelling the Flying Bird*, Academic Press, Academic Press/Elsevier, 2008. URL https://books.google.com.co/books?id=hHsYlQEACAAJ.

APPENDIX A. WEIGHTS, MEASURES, AND PERFORMANCE DATA

sectionAppendix

A. Weight, measures and performance data

1. Rocket airframe

Parameter	Value
Nosecone length	60 cm
Nosecone outer diameter	11.4 cm
Nosecone tickness	0.24 cm
Body tube length	187 cm
Body tube diamater	11.4 cm
Body tube thickness	0.25 cm
Fin height	10 cm
Fin root chord	25 cm
Fin tip chord	10 cm
fin tichkness	0.6 cm
Liftoff weight	14.6 kg

Table 7 Rocket airframe parameters

2. Flight data

Parameter	Value
Maximum velocity	343 m/s
Launch rail departure velocity	34.6 m/s
Maximum acceleration	153 m/s^2
Liftoff thrust-weight ratio	10
Apogee	2910 m

Table 8 Flight data

3. Motor performance

Parameter	Value
Average Thrust (N)	1915
Impulse (NS)	4999
Type	L
Delivered IPS (s)	127.36
Burn time (s)	2.58
Average Pressure (psi)	980
Propellant Mass (Kg)	4
Grain diameter (mm)	82
Grain length (mm)	165
Grain core (mm)	29
Material	AISI 304
Min Wall Thickness (mm)	4
Throat Diameter (mm)	16
Exit Diameter (mm)	50.46
Convergence Half Angle	30
Insulation Thickness (mm)	1

Table 9 Motor Characteristics.

APPENDIX b. HAZARD ANALYSIS APPENDIX

Table 10 Hazard Analysis

Orion Mission	**3/07/2022**		
Possible Causes	**Risk of Mishap and Rationale**	**Mitigation Approach**	**Risk of Injury after Mitigation**
Igniter does not fire	Medium. Electronic circuit does not function properly	1) Test ignition device before launch until reduce errors at minimum 2) Standardize ignition procedure	Low.
Center of pressure over center of gravity	Low. Discordance between theoretical and real model	1) Verify liftoff weight after manufacturing rocket 2) Verify center of mass position after manufacturing rocket	Low
Weak thrust retention	Medium. Bad design of thrust retention plate.	1) Resistance calculation of thrust retention plate	Low.
Parachute is not ejected or is misfunctioning	Medium. Lack of redundancy in electronic devices and tests.	1) Apply redundancy algorithms for deploying parachute 2) Test deployment hardware for reducing possible mistakes	Low

APPENDIX C. RISK ASSESSMENT

Table 11 Risk Assessment

Team 39	**Orion Mission**	**3/07/2022**		
Risk	**Possible Causes**	**Risk of Mishap and Rationale**	**Mitigation Approach**	Low.
Motor ignition before launch near people	Accidental source of heat near motor storage	Low. Lack of protocol for propellant storage	1) Warning marks 2) Predefined place and mode of storage	Low.
People around an unstable rocket after liftof	Center of pressure over center of gravity	Low. Discordance between theoretical and real model	1) Follow procedures established for LASC related to distance between launchpad and people at the event 2) Add a condition to the algorithm for activating deployment hardware if rocket presents high angles of attack	Low.
Rocket airframe or motor fall over people	Weak mechanical resistance of pieces or parachute does not open	Medium. Bad design procedures	1) Verify engineering calculations 2) Test rocket airframe resistance 3) Safeguard people under marquees	Low.